Water Practice & Technology

IWA PUBLISHING

Water Practice & Technology Vol 19 No 3, 1032 doi: 10.2166/wpt.2024.036

The effect of the compound slope spillway on air entrainment and total kinetic energy using computational fluid dynamics

Udai A. Jahad [a,*], Mohammed A. Alabas[b], Ammar Shaker Mahmoud[b], Riyadh Al-Ameri[c] and Subrat Das[c]

[a] Department of Environment Engineering, College of Engineering, University of Babylon, Babylon 51001, Iraq
[b] Department of Civil Engineering, College of Engineering, University of Babylon, Babylon 51001, Iraq
[c] School of Engineering, Faculty of Science Engineering & Built Environment, Deakin University, 75 Pigdons Road, Waurn Ponds, VIC 3220, Australia
*Corresponding author. E-mail: eng.udai.jahad@uobabylon.edu.iq

UAJ, 0000-0002-7041-5784

ABSTRACT

The spillway is a hydraulic structure used for managing discharge, dissipating energy, and aeration purposes. The objective of this CFD analysis was to compare the ways in which water moved over various slanted spillways. Both the turbulence and the air–water interface were located using the volume of fluid (VOF) technique and a realizable k-model. Five different spillway models with varying slopes (normal = 30°, compound1 = 20° and 39°, and compound2 = 39° and 20°) were modelled and simulated in ANSYS Fluent. Computational data have been compared to the experimental results, and the findings were astonishing – the CFD model precisely captured the all-important flow facets. The numerical model pinpointed the inception point that occurred due to changes in slope and structure. In comparison to the normal slopes of (30°) and the compound slopes of (39°/20°), the surge in the location of the inception point was around 58%. The results of the research indicate a significant increase in turbulent kinetic energy as a result of the introduction of the compound slope. The study conducted has effectively achieved a crucial objective of the project, which is to enhance the operational efficiency and reliability of the spillway under diverse flow conditions.

Key words: air entrainment, CFD, compound slope, inception point, spillway

HIGHLIGHTS

- Use the CFD to simulate the flow over the spillway with a compound slope.
- Study the impact of compound slope on the inception point.
- Investigate the slope effect on longitudinal velocity.
- Study the impact of slope on turbulent kinetic energy.

GRAPHICAL ABSTRACT

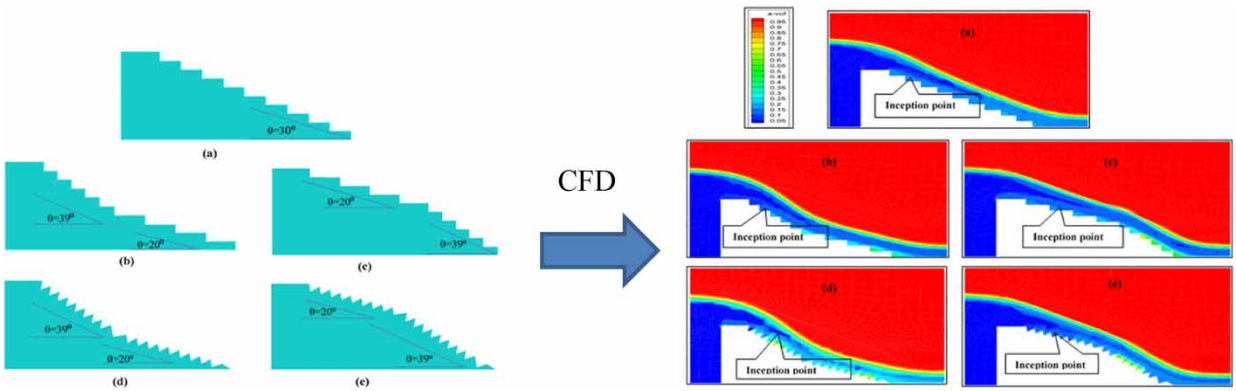

1. INTRODUCTION

One of the most important challenges in the performance of hydraulic structures is their stability and safety. One way of addressing this concern is through the use of spillways. Such a structure serves to dissipate energy from the water flow, thus decreasing the size of the stilling basin and reducing the potential for cavitation. In addition, the spillway improves the aeration of the water, leading to an increase in the concentration of dissolved oxygen (DO), which further enhances the safety of the structure. Spillways are often a preferred solution for the release of excess water from a reservoir due to their twofold ability to dissipate energy and aerate the water. By introducing steps into the spillway, the size of the hydraulic jump in the stilling basin is reduced, leading to a corresponding reduction in the basin's length. This allows for fast and efficient elimination of excess energy. Additionally, these steps create a certain degree of turbulence, increasing the boundary layer and thus allowing more air to flow along the spillway and the free surface. This reduces the risk of cavitation damage, a common problem in spillways. Moreover, factors such as roughness height and location have a determining influence on the thickness of the boundary layer. Steps thus serve not only to promote better energy dissipation but also more uniform flow conditions. In the long run, stepped spillways help to minimize water loss and thus maximize efficiency (Tian *et al.* (2022).

The boundary layer of the turbulence which exists in the water body ultimately reaches the free surface, which is known as the surface inception point. This point can vary greatly depending on the location, with places experiencing higher levels of turbulence more likely to see an earlier inception point at the surface. As the turbulence advances closer to the free surface, it also increases in intensity, creating large fluctuations in pressure, total kinetic energy, and other variables (Puri *et al.* 2023). Also, when the surface of a body of water is disturbed enough to break up the surface tension, it creates a phenomenon called aeration. This aerated zone gradually gets thicker and more scattered as the current of air spreads outwards. In the case of the spillway with a stepped slope, this aeration process can be extended all the way to its furthest edges, where the gas pockets created in the water are ultimately dispersed and the aerated area has reached its full depth. This phenomenon is visible in the way the water changes its colour and texture. Bubbles form on the surface, and it may even appear to ripple like that of foam. This aeration process has numerous implications for water ecology, including but not limited to the reintroduction of oxygen into the water, and improved circulation of water (Zhang & Chanson 2016). According to Xu *et al.* (2021), the phenomenon of the pseudo-bottom inception point is impactful, as it provides an effective way to measure the cavitation potential of stepped spillways. This point allows engineers to define and measure the air concentration precisely, which allows for the selection of the appropriate steps to minimize the impact of cavitation in a spillway. The exact position of the pseudo-bottom inception point must be determined carefully depending on the individual characteristics of each stepped spillway, and proper calculation of these points is crucial to ensuring that the cavitation potential of a spillway is accurately measured.

Air entrainment in spillways is an effective way to manage water control measures due to the combination of entrained and trapped air, which leads to the total absorption of air (Kramer *et al.* 2020). One key point of consideration is the upstream inception point of the stepped spillway, as this can determine the risk of cavitation (Shahheydari *et al.* 2015). The area at the inception point is closer to the bottom than it is in smooth spillways, making it more efficient in terms of aerated flows (Roushangar *et al.* 2020). The combined with reduction of drag due to the merging of air bubbles and layers, results in less energy dissipation in the white-water flow (Daneshfaraz & Ghaderi 2017). Bung & Valero (2018) stated that hydraulic structures affect the gas transfer dynamics of white water, with DO being the most important parameter related to the quality of rivers and streams. In particular, these structures alter the substrate surface characteristic, which consequently affects the ratio of exchange gases like DO. Thus, the presence of these structures influences the water quality in the vicinity. According to Roy *et al.* (2021), hydraulic structures (such as channels) can create turbulent conditions which lead to an increase in DO levels. This is due to air bubbles, particularly small ones, being transported into the main flow from the chutes of the structures as a result of the aeration process. All the above factors make stepped spillways a better choice for the safety of water control measures when compared to non-aerated ones (Stojnic *et al.* 2021).

The spillway's downstream slope is an essential part of its overall design and construction. It is determined by dividing the entire elevation of the channel by the length of the channel, or by dividing the step height by the step length. Stepped spillways can be classified as either 'mild' (with a slope of 10–14°), 'moderate' (with a slope of 14–22°), or 'steep' (with a slope higher than 22°). Spillways are more reliable and less prone to silt build-up from high flow rates if they have steeper gradients (Valero & Bung 2016). Moreover, according to

Wang *et al.* (2022), the downstream slope of the spillway affects its function and ultimately, the constructability of the spillway. For all these reasons, the downward slope of the spillway must be carefully considered when designing any type of spillway. It is also vital to review the spillway structure during construction to verify that the desired slope is correctly implemented. Additionally, as the slope increases, the spillway should be assessed to ensure it operates safely. Ultimately, the design, construction, and performance of the spillway will depend largely on the downstream slope that has been chosen.

In previous studies, numerical modelling has been used (for example, Barzegari *et al.* 2019; Saidin *et al.* 2020; Gu *et al.* 2022; Ramya & Kumar 2023). An extremely significant and widely used method in many engineering domains is numerical modelling. Computational fluid dynamics (CFD) is one specific illustration of a numerical technique. Hydraulic engineers have begun using this technique more frequently to develop intricate spillway designs and constructions. The main benefit of CFD is that there is no need to create a physical prototype or model, which saves a lot of work, money, and resources (Nóbrega *et al.* 2022). Hydraulic engineers should use CFD since physical modelling is a time-consuming and expensive process to carry out. CFD is advantageous because it can provide a precise full-flow description. The increased interest in CFD indicates that this method is proving to be both time and cost-effective and is being incorporated into the design processes of many hydraulic engineers (Bayon *et al.* 2018).

Numerical simulation of the flow over spillways is a challenging task owing to the dynamic nature of the flow. The utilization of the Reynolds-Averaged Navier–Stokes (RANS) method in conjunction with other turbulence simulation models, such as Reynolds stress models (RSMs), proves to be an effective approach for investigating flow regimes of this nature. Recent studies have revealed that the geometry of a stepped spillway is also a crucial parameter that can significantly influence the flow pattern and is, therefore, a critical decision factor in the design and construction of any type of stepped spillway (Lopes *et al.* 2017). Furthermore, the incorporation of air entrainment phenomena produces an additional complexity in the skimming flow regime over stepped spillways. Due to the methodological advantages, RANS coupled with RSMs is the way to go for simulating such complex flows with considerable accuracy (Pedersen *et al.* 2018).

Wan *et al.* (2019) used many models to investigate the correlation between the dam's incline, the ogee of the spillway bottom, and the amount of energy lost. It was determined that there would be a proportional increase in energy loss as the spillway level rose. Moreover, their findings suggested that stepped spillways without an ogee lost a lot more energy than those with an ogee at the spillway's foot. Several models were used to analyse the turbulence and shed light on the features of turbulent flow on the stepped spillways. Dong *et al.* (2019) simulated a stepped spillway model and compared the results to those obtained using the RNG (renormalized group) k-model. The RNG turbulence model was shown to provide a more precise depiction of the flow's behaviour than the traditional k-model. This exemplifies how turbulence modelling is crucial for the most accurate analysis of stepped spillway models using CFD. Also, the compound slope spillways often encounter challenges related to air entrainment and the management of total kinetic energy. Air entrainment can lead to reduced flow efficiency and increased turbulence, impacting the spillway's functionality and potentially causing erosion or structural problems. CFD is essential in studying these issues as it allows for in-depth analysis of flow patterns, turbulence, and the interaction between air and water, aiding in designing more effective spillway structures to mitigate these problems (Muhsun *et al.* 2020).

Using CFD, this research looks at how the slope of a spillway's complex affects air entrainment and where it begins. It was determined by experimenting with four various slopes (300, 390/200, and 200/390) how the size of the non-aerated flow region changes as the slope changes. Fifteen simulations were run using Fluent Software and the Volume of the Fluid model, with each model simulated at five different discharge rates. Each simulation scenario's turbulence influx was computed using the realizable k-model. In order to examine the connection between slope, non-aerated flow zone length, inception point, and discharge, the simulation results were put through a series of mathematical operations.

2. MATERIALS AND METHODS

2.1. Air entrainment

Aeration is a procedure of exchanging air between the water body and the atmosphere. This helps to increase the DO in the water column. It is beneficial for aquatic life as it increases circulation and flushes out pollutants. Additionally, aeration improves the mixing of different layers of water. All these effects together lead to improved

water quality (Fu *et al.* 2019). Moreover, the gas transfer is an important element of water quality, especially in white water. The presence of oxygen is the most crucial parameter to determine water quality as it can reveal the presence of other pollutants like nitrogen, chlorine, volatile organic compounds, and methane. When the oxygen concentration is low, these harmful impurities can be detected. These compounds are produced due to the breakdown of organic matter in water. As a result, it's essential to closely monitor water quality so that it is safe for people to use.

Assessing the flow of gases, such as oxygen, at the interface between air and water involves numerous factors that must be considered. As oxygen molecules are relatively small, they can pass through the airspace leading to the water with relative ease, meaning that they can usually be found in the liquid phase in different concentrations. The gas flow might be calculated as follows:

$$\frac{dC}{dt} = k_{\mathrm{L}} \frac{A_{\mathrm{s}}}{\forall} (C_{\mathrm{s}} - C) \tag{1}$$

where 'the rate of change in concentration (dC/dt) is dependent on the surface area of bubbles (A_{s}), the volume of water in which C and as are measured ($\forall$), the DO concentration in water (C), the saturation concentration of oxygen in water (C_{s}), the liquid film coefficient (k_{L}), and time (t)'.

According to Srinivas & Tiwari (2022), if the saturation concentration C_{s} remains the same throughout time, then aeration efficiency (EO) may be quantitatively described as follows:

$$\mathrm{EO} = \frac{\boldsymbol{C}_2 - \boldsymbol{C}_1}{\boldsymbol{C}s - \boldsymbol{C}_1} \tag{2}$$

where C_1 represents the DO concentration at the upstream of the hydraulic structure and C_2 represents the DO concentration at downstream. Temperature can influence the efficacy of aeration. Historically, a temperature correction factor has been utilized to calculate the impact of temperature. This relationship is elucidated in the following equation:

$$\mathrm{EO}_{20} = 1 - (1 - \mathrm{EO})^{(1/\mathrm{ft})} \tag{3}$$

The aeration efficiency (EO) can be represented by the aeration efficiency at 20 °C (EO20) and an exponent (f) as described by Equation (4). This equation provides an accurate representation of the efficiency of the aeration process:

$$f_t = 1.0 + 0.02103(T - 20) + 8.261 \times 10^{-5}(T - 20)^2 \tag{4}$$

where T is the water temperature.

2.2. CFD model setup

As a subfield of fluid dynamics, CFD uses numerical calculations and various data formats to address a wide range of practical flow problems. The Navier–Stokes equations provide the theoretical foundation for this. Although they are more time-consuming and resource-intensive than the finite volume method, finite element and finite difference approaches are frequently used for the analysis of solid structures. By partitioning the full volume of interest into smaller sets of volumes, the Navier–Stokes equations, the primary differential equations, may be solved using the finite volume approach. The Navier–Stokes equations are discretized using the finite volume method in the fluent programme. The flexibility of the finite volume approach makes it an attractive choice since it simplifies the creation of unstructured meshes.

The current study investigates the flow characteristics of four different types of spillways, of varying inclines, using numerical modelling with the aid of the software Fluent. All four spillways (as shown in Figure 1) employ the multi-phase volume of fluid (VOF) methodology, along with the realizable k-ε turbulent model, as determined from literature analysis to be the most effective boundary layer approach. SIMPLE algorithms are also incorporated for coupling velocity and pressure during transient simulations. Furthermore, second-order upwind schemes are applied towards the momentum, with pressure-staggered solutions used for the turbulent kinetic energy (TKE) dissipation rate. All the spillways have the same width (0.5 m) and the slopes as seen in

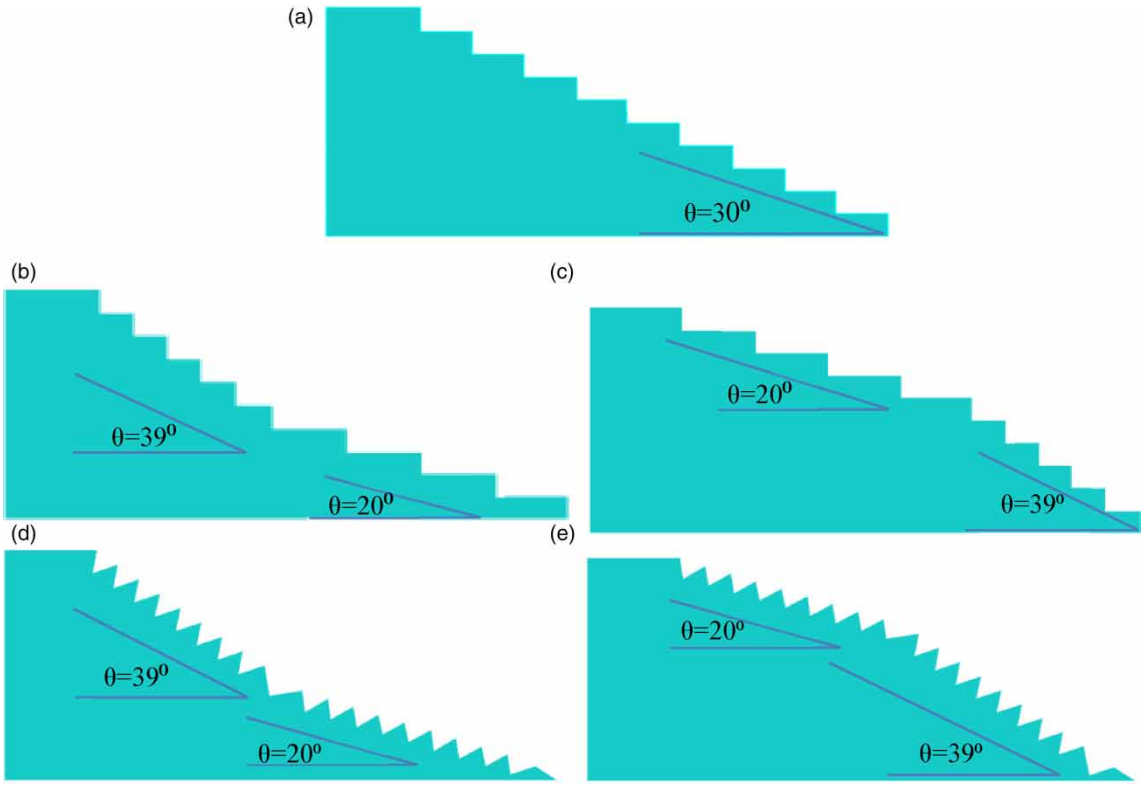

Figure 1 | Geometry of the model, (a) SS1, (b) SS2, (c) SS3, (d) SS4, and (e) SS5.

Table 1. In order to further understand the flow dynamics, the behaviour of the boundary layer along the spillways is of particular interest to this study. To measure this, the computation of velocity and turbulent intensity along the spillways will be included in the numerical model. These values will then be visualized and analysed for differences between the four different models, in order to make predictions and gain insights into the efficacy of each for different inclines. With the help of the software and numerical modelling, it is hoped to gain a better understanding of the flow characteristics of stepped spillways and gain information that can contribute to their future use.

Table 1 | The size of the CFD models employed

Model#	θ°	Model height (h_d) cm	Crest length (l_c) cm	Step length (l) cm	Step height (h) cm	Step number (N)
SS1	30	30	10	5	3	10
SS2	39/20			8/4		5/5
SS3	20/39			4/8		5/5
SS4	39/20			3		9/9
SS5	20/39			3		9/9

2.3. CFD equations

The techniques of CFD have been identified as a cost-effective alternative for experimenters. The software ANSYS Fluent is able to simulate the fluid flow over spillways in a numerical format. Utilizing this program, experimenters can render highly accurate results that require fewer resources and less time. The extensively used equations in CFD are the RANS equations. These equations are partial differential equations, meaning they display the motion of the fluid. Generally, these equations are outlined using the common k turbulence model. The mass equation (Equation (5)) is a fundamental part of physics, as it provides a description of how

different bodies are related to one another in terms of their mass:

$$\frac{\partial \rho}{\partial t} + \frac{\partial \rho u_i}{\partial x_i} = 0 \tag{5}$$

$$\frac{\partial \rho u_i}{\partial x_i} + \frac{\partial}{\partial x_i}(\rho u_i u_j) = -\frac{\partial p}{\partial x_i} + \frac{\partial}{\partial x_j}\left\{\mu\left(\frac{\partial u_i}{\partial x_j} + \frac{\partial u_j}{\partial x_i} - \frac{2}{3}\delta_{ij}\frac{\partial u_k}{\partial x_k}\right)\right\} + \frac{\partial}{\partial x_j}(-\rho u_i' u_j') \tag{6}$$

where 'ρ is the density of the fluid, μ is molecular viscosity, u_i is the velocity component, x_i is the coordinate component, t is the time, and p is the pressure. The deviatoric stress component in Equation (7) can be expressed as:

$$\rho u_i' u_j' = \mu_t\left(\frac{\partial u_i}{\partial x_j} + \frac{\partial u_j}{\partial x_i}\right) - \frac{2}{3}(\rho k)\delta_{ij} \tag{7}$$

where 'μ_t is the turbulent viscosity and the stress tensors $\delta_{ij} = 1$ when $i = j$ and $\delta_{ij} = 0$ when $i \neq j$, using the k-ε model for turbulence closure' (Torrano *et al.* 2015):

$$\frac{\partial(\rho k)}{\partial t} + div(\rho k U) = div\left\{\left(\frac{\mu_t}{\sigma_k}\right) grad k\right\} + 2\mu_t E_{ij} E_{ij} - \rho\varepsilon \tag{8}$$

$$\frac{\partial(\rho \varepsilon)}{\partial t} + div(\rho \varepsilon U) = div\left\{\left(\frac{\mu_t}{\sigma_\varepsilon}\right) grad \varepsilon\right\} + C_{1\varepsilon}\frac{\varepsilon}{k} 2\mu_t E_{ij} E_{ij} - C_{2\varepsilon}\rho\frac{\varepsilon^2}{k} \tag{9}$$

$$\mu_t = \rho\, C_\mu \frac{k^2}{\varepsilon} \tag{10}$$

where $C_u = 0.09$, $\sigma_k = 1.0$, $\sigma_\varepsilon = 1.3$, $C_{1\varepsilon} = 1.44$ and $C_{2\varepsilon} = 1.92$.

2.4. Mesh and the boundary conditions

Representing the domain of the geometry of air–water flow, two meshing approaches have been put forth for consideration: structured mesh and unstructured mesh. Ultimately, which has the greatest performance is impossible to determine without assessing each individual case on its own merits. Zawawi *et al.* (2018) point out that the unstructured mesh is advantageous due to its ability to selectively refine areas of smaller gradients and its multi-component geometry. Moreover, the arbitrary topology of the unstructured mesh makes automating the meshing process easier and the closure of the mesh is fewer. In order to accurately capture the flow features in the boundary layers, a refinement of the mesh is necessary. This can lead to a deformation of the elements, but this is not an issue as long as the mesh axes are kept perpendicular to the solid boundaries. Based on this principle, it is recommended to use a structured rectangular hexahedral mesh for the present study involving CFD work. To ensure optimized results, it is also beneficial to implement inflation layers into the mesh. Low-complexity geometry (a rectangular channel) and high-complexity geometry (flow over a spillway) were compared. We chose a 2 mm mesh and a 3 mm element size for the low-complexity geometry, with no inflation layers. However, a mesh size of 1 mm, an element size of 2 mm, and 10 inflation layers were needed to accurately model the extremely complicated geometry. As an example, the mesh for the SS1 model is seen in Figure 2; this part of

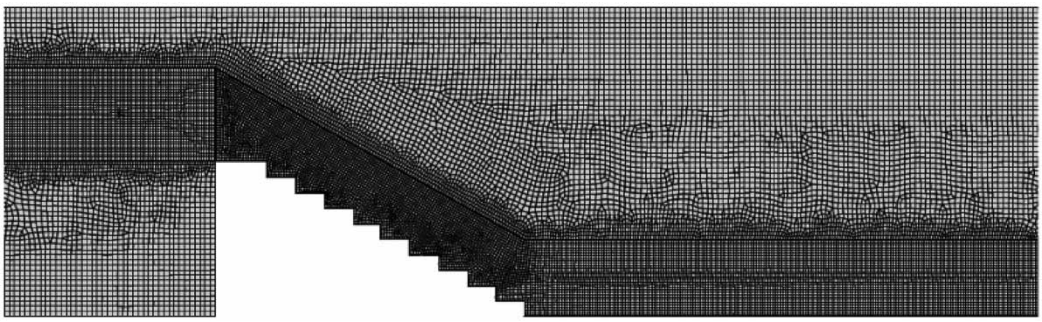

Figure 2 | The mesh and inflation layers of SS1 model.

geometry shares the same dimensions as the actual physical model. There were a total of 368,490 elements and 369,709 nodes.

For spillway models, the inlet boundary conditions include a velocity inlet that changes with the flow rate. The speed at which the spillway is being pushed rises in proportion to the volume of water passing through it. As a result, the velocity applied at the intake of spillway models varies with the discharge rate. Using continuity equations, the speed was calculated for five experimentally observed discharges ($Q = 4.35$, 10.10, 25, 38.46, and 55.55 L/s). The pressure outlet of a spillway is located at the point when backwater flow is zero. The backwater flow from the outflow has little significance as a result. The walls of the spillway have zero kinetic energy and are thus immovable. This creates a static environment that is vital to the functioning of the spillway.

3. RESULTS AND DISCUSSION

Four models of spillways, varying in steepness from mild to steep, are simulated using the VOF and k-realizable models. The simulation was designed to determine the slope-specific inception point and non-aerated flow length. Discharge rates ($Q = 4.35$, 10.10, 25, 38.46, and 55.55 L/s) were modelled at 30°, 39°/20°, and 20°/39° spillway slopes. The purpose of this experiment is to determine how the channel slope of the spillway affects the inception points and the length of the non-aerated flow zone.

3.1. Model validation

The Deakin University study team used a flume that was 7.0 m in length, 0.5 m in width, and 0.6 m in depth for their in-laboratory studies. The discharge rate (Q) was measured in the flume using a flowmeter with a precision of 1 L/s. The downstream spillway velocity (V1) was measured using a 3 mm diameter plastic incurved Prandtl–Pitot tube. Instrumental error was kept to a minimum of 0.2 mm by installing the tube at an angle of 30° and using a digital gauge system to enhance precision. In addition, a horizontal beam placed at a considerable distance from the tube served to stabilize it and lessen vibration when the flow rate was high. Non-aerated flow velocities were determined using Prandtl–Pitot tube findings (Jahad *et al.* 2022).

The experimental data were used to accurately measure the velocity downstream of the spillway and verify the CFD simulations conducted. Compliance testing with Equations (11) and (12)'s root mean square error (RMSE) and mean absolute percentage error (MAPE) were used to assess the accuracy of the model and to acquire data to back up the CFD results. Subsequently, these collected data were compared and assessed against the experimental outcomes. This process of comparison and validation provides critical evidence to support the use of CFD simulations, which allows engineers to use these models without any doubts concerning their reliability. This bottom-up approach is essential in ascertaining accurate CFD results during the engineering process. It is a practical and feasible way to acquire and validate results, while also providing confidence and assurance in the modelling outcomes:

$$\mathrm{RMSE} = \sqrt{\frac{1}{n}\sum_{1}^{n}(\mathrm{V1}_{\mathrm{experimental}} - \mathrm{V1}_{\mathrm{CFD}})^2} \tag{11}$$

$$\mathrm{MAPE} = 100 * \frac{1}{\mathrm{n}}\sum_{1}^{n}\left|\frac{\mathrm{V1}_{\mathrm{experimental}} - \mathrm{V1}_{\mathrm{CFD}}}{\mathrm{V1}_{\mathrm{experimental}}}\right| \tag{12}$$

In addition to correlating the results, the correlation coefficient R was also used to assess the accuracy of the experiment and results obtained from CFD. The comparison of the experimental values with those obtained from the CFD model was revealed in detail in Figure 3. The velocity of flow, V1, was used as the parameter of analysis. Three indicators were used to evaluate the accuracy of the model, RMSE, R, and MAPE. The results showed a MAPE of 4.31, an RMSE of 0.20, and an R-value of 0.984. These close-to-zero values of the RMSE demonstrate the precision of the CFD model in comparison to the experimental values, thus providing strong evidence for its effectiveness and accuracy. Furthermore, it was also observed that within a short period of time, satisfactory results can be obtained. In conclusion, this study showed the reliability, effectiveness, and accuracy of the CFD model as compared to experimental data. Therefore, its use can be encouraged in cases where accurate results are needed in the least amount of time.

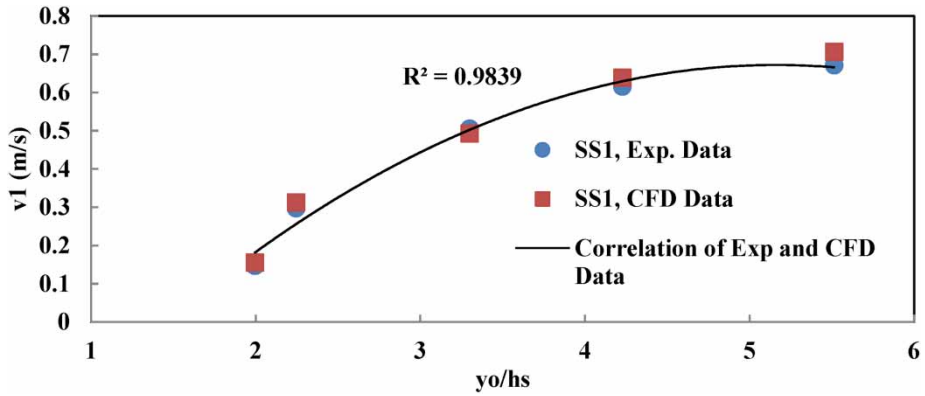

Figure 3 | The relationship between the experimental and CFD models.

3.2. The impact of compound slope on the inception point

The proper selection of the compound slope of spillways is an essential factor in determining its performance. Correct channel slopes can help to find the exact location of the inception point and the size of the non-aerated flow zone. As illustrated in Figure 4, increasing the channel slope leads to a slower ascent of the inception point, and a decrease in the size of the non-aerated flow zone when compared to all discharges. Table 2 shows the outcomes of this decreased non-aerated flow zone and Froude number fluctuation. Channel slope, surface roughness, Froude number, and step height are all related in this table. The Froude number (as indicated by Equation (13)) is affected by the surface roughness of the stepped spillway, which develops in proportion to the slope. All these parameters must be considered for the purpose of optimal design of a spillway. Therefore,

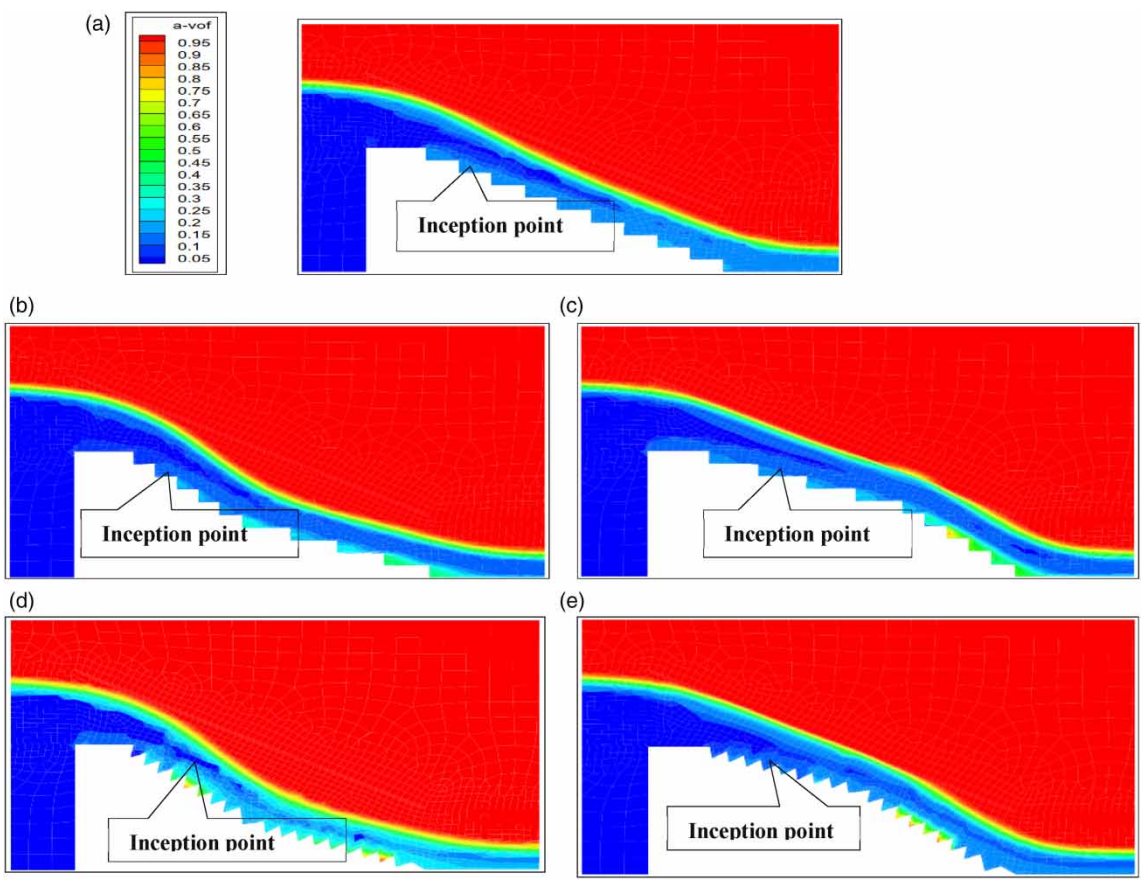

Figure 4 | The length of inception (L_i) at $q = 0.050$ (m^3/s)/m.

Table 2 | The predicted data for the inception point for CFD models

Model	$q \times 10^{-2}$	θ°	h (cm)	L_i (cm)	Fr^*	K_s	L_i/K_s
SS1	0.87	30	3	1.40	0.94	0.026	0.54
	2.02		3	2.55	2.18	0.026	0.98
	5.00		3	5.67	5.39	0.026	2.18
	7.69		3	6.35	8.28	0.026	2.44
	11.11		3	7.75	11.97	0.026	2.98
SS2	0.87	39/20	3	3.44	1.01	0.028	1.23
	2.02		3	5.66	2.35	0.028	2.02
	5.00		3	9.27	5.83	0.028	3.31
	7.69		3	11.73	8.96	0.028	4.19
	11.11		3	12.74	12.95	0.028	4.55
SS3	0.87	20/39	3	3.18	0.99	0.023	1.38
	2.02		3	6.05	2.31	0.023	2.63
	5.00		3	10.52	5.71	0.023	4.57
	7.69		3	12.59	8.78	0.023	5.47
	11.11		3	16.08	12.69	0.023	6.99
SS4	0.87	39/20	3	3.72	1.01	0.028	1.33
	2.02		3	7.08	2.35	0.028	2.53
	5.00		3	12.31	5.83	0.028	4.40
	7.69		3	14.74	8.96	0.028	5.26
	11.11		3	18.82	12.95	0.028	6.72
SS5	0.87	20/39	3	2.01	0.99	0.023	0.87
	2.02		3	4.89	2.31	0.023	2.13
	5.00		3	10.90	5.71	0.023	4.74
	7.69		3	13.34	8.78	0.023	5.80
	11.11		3	17.54	12.69	0.023	7.63

understanding the effects of the channel slope is important for ensuring the efficient and successful operation of the facilities:

$$F* = \frac{q}{\sqrt{g \sin \emptyset \, k_s^3}} \tag{13}$$

where $k_s = h \cos(\theta)$.

Discharge (q) is directly proportional to the inverse of the distance (L_i) from the top of the spillway to the point of inception. This can be observed in Figure 5 and clearly displays that the discharge has a direct influence on the inception length. When the discharge is higher, the corresponding inception length is greater. This finding confirms a previous study by Wan *et al.* (2019) which has suggested that higher discharges indicate larger inception lengths. Moreover, it appears that the inclination and discharge can have an interactive effect on the inception length. Regardless of the variation in slopes, the highest discharge always demonstrated the longest inception length. This could be due to the relationship between water depth, velocity, and slope steepness. That is to say, when the discharge is higher, the water depth will be greater and the velocity can increase. This results in a rise of the shear stress, which can eventually lead to a longer inception length. At the same time, higher discharges may also decrease the response time of the channel reach to changes in slope, which contributes to the occurrence of longer inception lengths. This is further highlighted when the discharge is taken to its highest, resulting in a noticeable surge in inception lengths across all the conditions. This emphasizes the importance of exploring the key role of increasing discharges in governing inception length. Furthermore, it is also worth noting that the influence of increasing discharges is bound by a certain limit. While higher discharges lead to greater inception lengths, this effect is limited up to a certain point. This indicates that additional factors such as flow turbulence, and flow obstructions could impact the relationship between discharge and inception length. Overall, the trend of Figure 5(a) reveals that the discharge and inclination of the channel reach have an interdependent relationship with the inception length. Higher discharges typically signify longer inception lengths; however, this outcome is subject to a limit. Additionally, the interactive effect of the inclination and discharge suggests that the shear stress and response time of the reach may also be influential when studying influx length. As such, further research is needed to better understand the influence of all these factors.

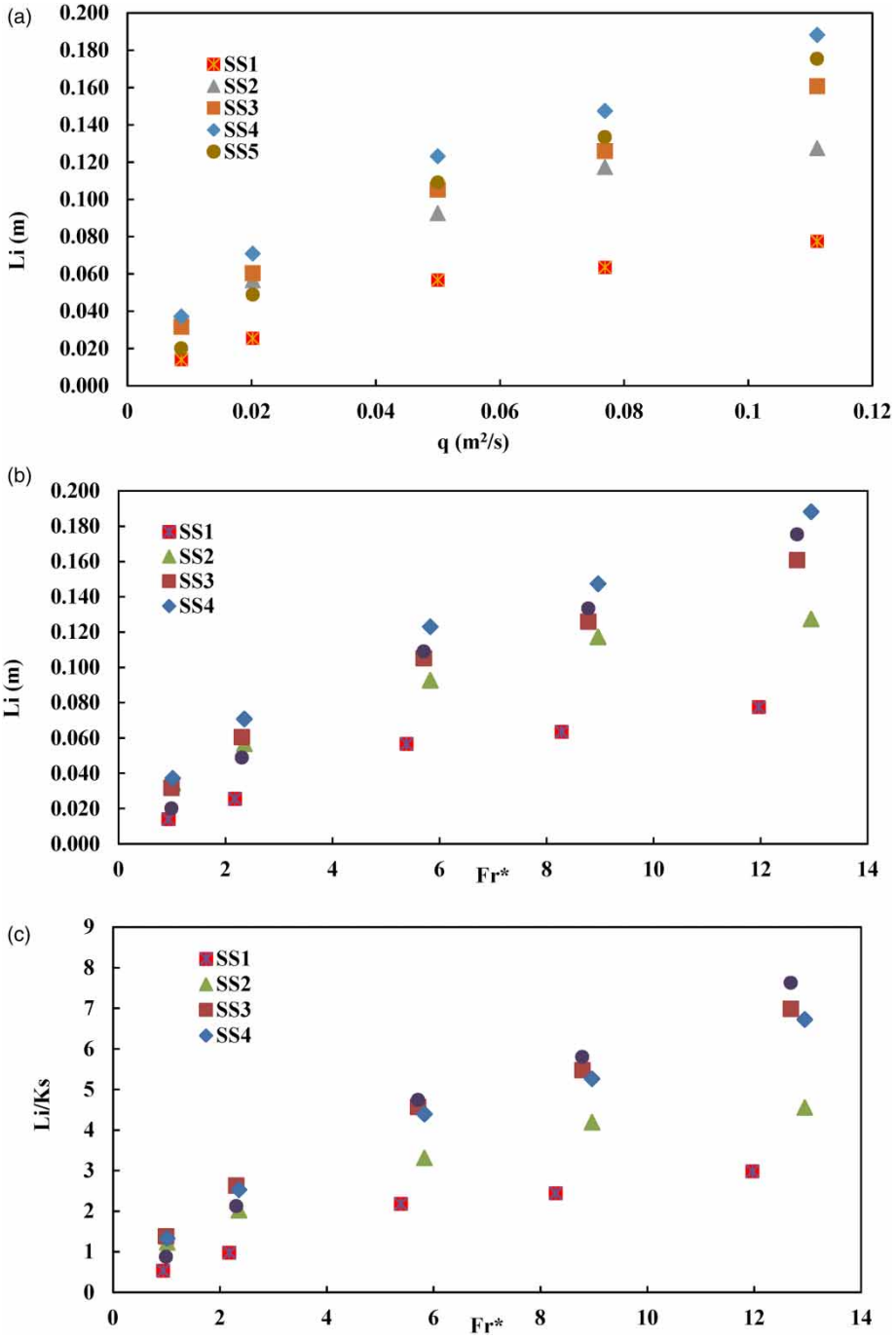

Figure 5 | (a) Discharge rate (q) against inception length (L_i) for several spillway models at varying gradients, (b) the inception length (L_i) and Froude surface roughness (Fr^*) relate to each other over a range of slopes for models of spillways, and (c) the relation between the normalized (L_i/K_s) with the Froude number of different slopes for spillway models.

The relationship between the inception length (L_i) and Froude surface roughness (Fr^*) is an important one, particularly in relation to the discharge with certain variations of roughness height. As shown in Figure 5(b), a direct correlation exists between the two, with an increase in Froude surface roughness resulting in an increase in inception length. This relationship is further evidenced by Equation (8), which states that an increase in discharge can cause the Froude surface roughness to spike. What is particularly interesting about this phenomenon is its variation in terms of the grade of the terrain. This is because the inception length will depend heavily on slopes, with steeper inclines resulting in an increased length. Consequently, variables including upstream channel geometry, channel shape, and channel material also play a role in determining the inception length. Ultimately, the

interplay between these variables, combined with the correlation between Froude surface roughness and inception length, allows for a more accurate model of the terrain and its connection to discharge and flow characteristics. If the Froude number rises to an abnormally high level, it may cause flow choking or make the spillway unable to manage the water volume, which will lower the flow velocity overall. That is to say, a small increase in the Froude number could indicate that the water is flowing efficiently and quickly, but an overly high number could cause flow instabilities or disruptions, which could lower the flow velocity over a spillway as a whole.

(L_i/k_s) is a parameter that mainly describes the distance from the crest to the point of origin for a given spillway. It can be calculated by taking the ratio of (L_i) to the surface roughness (k_s). It is observed that the normalized L_i decreases as the surface roughness (k_s) increases, therefore (L_i/k_s) is directly related to the Froude number. As the Froude number increases, so does (L_i/k_s), and a minimum value is observed for the least Froude number. Figure 5(c) provides a graphical representation of the variation of normalized (L_i) with the Froude number. It is important to note that with the increase in surface roughness (k_s), the normalized (L_i) will continue to be reduced leading to a decrease in the Froude number. As a result, it can be concluded that for greater spillway efficiency, the surface roughness k_s needs to be decreased such that the normalized (L_i/k_s) is maximized. This has many practical implications such as reducing scour and preventing flooding. Therefore, it can be said that understanding the correlation between the normalized (L_i/k_s) with the Froude number is fundamental for designing a spillway efficiently and allows for better control of water flow.

3.3. Slope effect on longitudinal velocity

Figure 6 demonstrates the diverse changes in the average longitudinal flow velocity over the spillway in terms of varying Froude numbers and ratios for $w/y_o = 1.32$. After passing through the crest from upstream, the flow velocity expands considerably and continues with almost a constant value downhill towards $x = 1.2$ m. After this point, there is a small further increase, and then the longitudinal velocity stays approximately consistent to the end section. The peculiarities of the velocity drop in different w/y_o ratios can also be observed in the figure. Even though the cross-sectional area of the flow that goes over the middle of the spillway is identical, there is no significant variance in the average velocity at different Froude numbers. This is probably due to the introduction of air to the flow, which enhances the flow velocity and makes it more energetic.

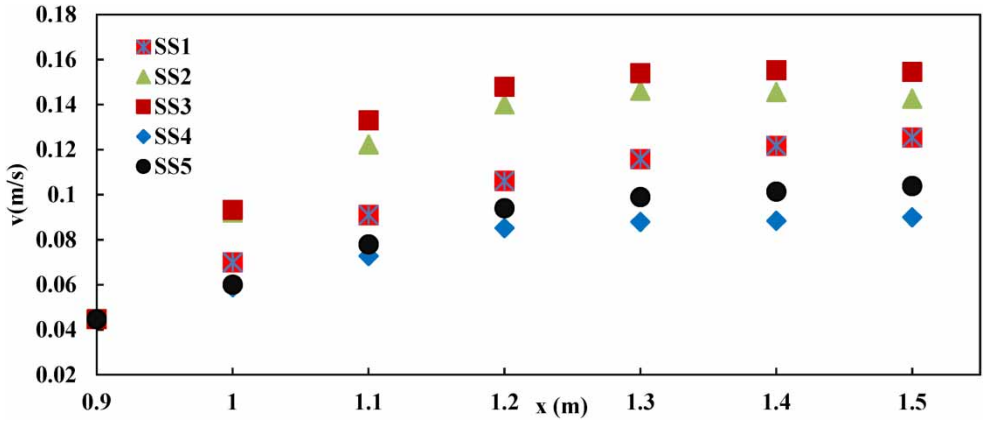

Figure 6 | The longitudinal velocity along the models' bodies for $w/y_o = 1.32$.

Furthermore, higher Froude numbers lead to a decrease in flow velocity, a sign that the friction of the walls and other surface interferences have a major effect on the flow. This causes higher turbulent diffusion of drive and energy, thus further diminishing the velocity. As further research is conducted on the topic of the influences that surface components have on the dynamics of liquid flow, it will become increasingly clear how the surface features can affect the flow patterns and properties.

3.4. The impact of slope on TKE

TKE is a common feature of the gradient of the velocity found in spillways. Extensive studies conducted on spillways with different discharges reveal that the variation of TKE follows a similar pattern. Also, The TKE is a key measure of the unpredictable and chaotic motion of water molecules during a turbulent flow, such as on a spillway. It describes the energy exchange between two points in the system and is an important factor in understanding the mean velocity gradients that lead up to it. TKE is a relevant concept in hydrodynamics and meteorology as it has an influence on various aspects of a turbulent flow. For example, it plays a part in how quickly a wave dissipates energy or how a particular dissolved gas eventually transfers to the atmosphere. As such, knowing the intensity of TKE can be beneficial in modelling how systems behave under different turbulent flow conditions (Bombardelli *et al.* 2011).

The findings of the TKE change process observed at $q = 0.050$ (m^3/s)/m have been especially revealing in highlighting the impact of step direction and downstream slope geometry on turbulent flow. As shown in Figure 7,

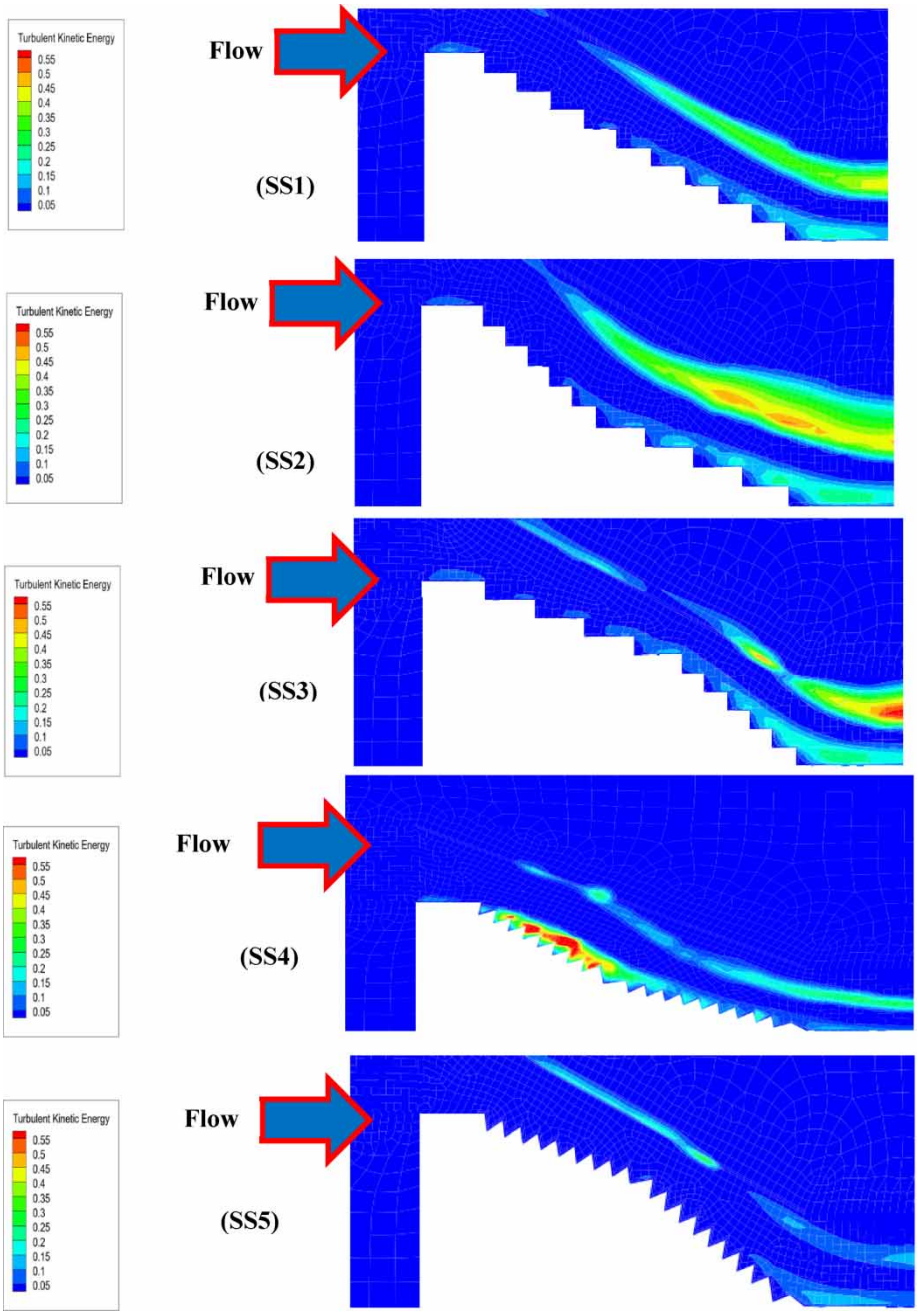

Figure 7 | Predicted TKE in different arrangement slopes for discharge $q = 0.050$ (m^3/s)/m.

increasing the downstream slope arrangement with step change can significantly increase the jet deflection on the steps and give the highest TKE at the compound slope of 18 steps for the model SS4. This suggests that such a configuration of step direction and downstream slope could be more effective in creating turbulence and energy dissipation in the selected application. Furthermore, Morovati & Eghbalzadeh's (2016) findings were supported as the TKE gradually increased along the spillway, indicating that the combined approach of changing the step direction and downstream slope arrangement is an effective method of increasing turbulence and energy dissipation for this particular discharge. Future studies will be required to verify the results of this procedure with different discharge rates in other applications. Additionally, further studies should consider the influence on TKE when the flow profile is altered, such as by using stepped chutes or terraced spillways. Different configurations will likely have varying levels of impact on TKE values, so further investigation could be undertaken to identify the most effective approach for each application.

Additionally, the TKE is shown in Figure 8 for the same discharge ($q = 0.050$ (m^3/s)/m) over spillways with varying slopes and numbers of steps. It is discernible from the diagram that for all the selected discharges, the most outstanding TKE values are seen in the spillway model SS3. Also, as the number of steps increases with slope changes, the TKE values decrease proportionally. With respect to the discharge rate, it is seen that higher discharges lead to higher amounts of TKE, as shown in the slope of the graph in Figure 8. It is steeper when the spillway has a slope (30°) as in the SS1 model suggesting the most significant decrease in the obtained TKW values for this section.

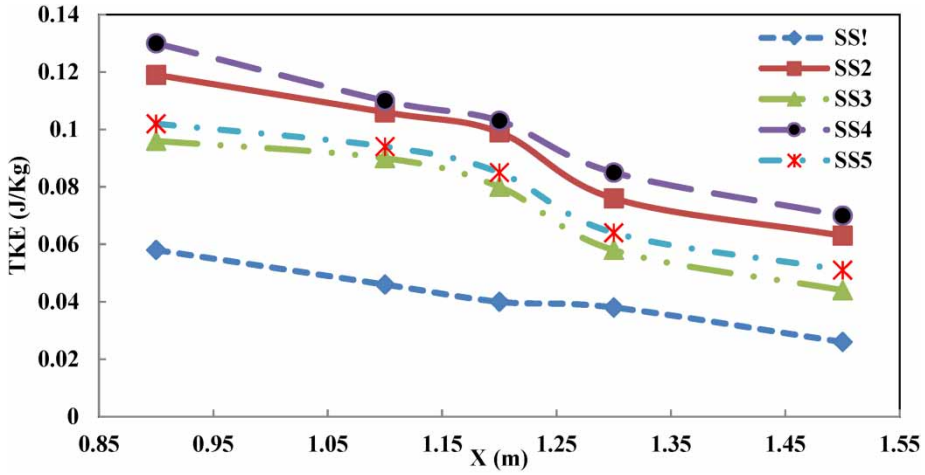

Figure 8 | The mean TKE on spillway with different slopes for discharge $q = 0.050$ (m^3/s)/m.

4. CONCLUSIONS

The downstream slope of spillways is crucial to their effective design, and it must be calibrated to the specific flow rate circumstances. The ANSYS Fluent Model, the VOF method, and the RNG-K turbulence model were used to conduct a numerical investigation of a stepped spillway with a compound slope to gain insight into this phenomenon. In order to evaluate the accuracy of the numerical simulation, an experimental investigation of a flat-stepped spillway was carried out. These results provide support for the idea that the compound slope parameters are controllable, opening the door to the safe and successful use of the stepped spillway. This study has important implications since it suggests that spillways may be able to adapt to a greater variety of flow circumstances if the downstream slope is modified. The results of this investigation show the following:

- The efficiency of numerical models, such as CFD, has been proven through various comparison studies. A recent study compared the CFD simulation of a large-scale water circulation model with a laboratory experiment. This suggests CFD is an accurate and reliable tool for predicting fluid flows.
- The location of the inception point for spillways is critical to its function and efficiency, as it is the point where the water starts flowing over the spillway. To accurately determine this inception point, the discharge, slope, and step geometry must be considered. It has been determined via study that the greater the discharge, the

farther the inception point is from the spillway's crest. Furthermore, there is a significant correlation between the distance to the inception point and the number of steps on the spillway. In contrast to steeper-sloped spillways, those with a typical slope have an inception point that is closer to the spillway crest. The Froude surface roughness (Fr^*) also plays a role in the location of the inception point. Generally, the higher the unit discharge, the higher the value of Fr^*, resulting in a longer distance to the inception point. It is important to take all these factors into consideration in order to design an efficient and effective spillway.

- Several simulations and comparisons were performed and examined to evaluate the five different types of spillway shapes. The study revealed that when the discharge and number of steps are held constant, the inception point of a spillway with a conventional slope and a normal step shape (referred to as the SS1 model) is situated closest to the crest of the spillway. Conversely, in spillways with compound slopes (specifically, the SS2, SS3, SS4, and SS5 models), the inception point is located farthest from the spillway crest. Furthermore, the data analysis revealed that the inception point would move upstream when the discharge increases and downstream when the discharge decreases. Therefore, the different spillway forms can make the inception point change its location according to the amount of discharge.
- The SS4 model, which is a spillway that has a compound slope, offers the best protection against cavitation. This is due to the fact that the non-aerated flow zone in a compound slope spillway is significantly lower than that of a spillway with a flat form. This reduction in the non-aerated flow zone then reduces the probability of cavitation damage occurring. Furthermore, as the boundary conditions remain the same, the use of a compound-slope spillway is preferable, as the probability of cavitation damage is minimized. Therefore, when designing a spillway, it is better to have a compound slope to effectively reduce the probability of cavitation damage.
- The study conducted on compound slopes has revealed that they are capable of generating higher turbulence energy (TKE) in comparison to traditional sloping arrangements. The intensity of turbulence on such slopes is also greater. This has enabled a whole new approach in the field of spillway design and operation. With new insights into the hydraulic characteristics of compound slopes, engineers are now empowered to alter the downstream gradient in order to meet flow rate requirements.

While this newfound knowledge base is quite extensive, it is far from exhaustive. Currently, it still remains unclear as to the intricate hydrodynamic consequences of designing compound slopes. Comprehensively understanding this aspect would provide the fundamental infrastructure for more precise and accurate engineering decisions. Furthermore, it opens the windows for additional investigations that can further our current understanding of spillway design and operation.

DATA AVAILABILITY STATEMENT

All relevant data are included in the paper or its Supplementary Information.

CONFLICT OF INTEREST

The authors declare there is no conflict.

REFERENCES

Barzegari, M., Sobhkhiz Foumani, R., Isari, M., Tarinejad, R. & Alavi, S. A. 2019 Numerical investigation of cavitation on spillways. A case study: Aydoghmush dam. *Numerical Methods in Civil Engineering* **4**(1), 1–9.

Bayon, A., Toro, J. P., Bombardelli, F. A., Matos, J. & López-Jiménez, P. A. 2018 Influence of VOF technique, turbulence model and discretization scheme on the numerical simulation of the non-aerated, skimming flow in stepped spillways. *Journal of Hydro-Environment Research* **19**, 137–149.

Bombardelli, F. A., Meireles, I. & Matos, J. 2011 Laboratory measurements and multi-block numerical simulations of the mean flow and turbulence in the non-aerated skimming flow region of steep stepped spillways. *Environmental Fluid Mechanics* **11**(3), 263–288.

Bung, D. B. & Valero, D. 2018 Re-aeration on stepped spillways with special consideration of entrained and entrapped air. *Geosciences* **8**(9), 333.

Daneshfaraz, R. & Ghaderi, A. 2017 Numerical investigation of inverse curvature ogee spillway. *Civil Engineering Journal* **3**(11), 1146–1156.

Dong, Z., Wang, J., Vetsch, D. F., Boes, R. M. & Tan, G. 2019 Numerical simulation of air–water two-phase flow on stepped spillways behind x-shaped flaring gate piers under very high unit discharge. *Water* **11**(10), 1956.

Fu, B., Merritt, W. S., Croke, B. F., Weber, T. R. & Jakeman, A. J. 2019 A review of catchment-scale water quality and erosion models and a synthesis of future prospects. *Environmental Modelling & Software* **114**, 75–97.

Gu, S., Zheng, W., Wu, H., Chen, C. & Shao, S. 2022 DualSPHysics simulations of spillway hydraulics: A comparison between single-and two-phase modelling approaches. *Journal of Hydraulic Research* **60**(5), 835–852.

Jahad, U. A., Al-Ameri, R. & Das, S. 2022 Investigations of velocity and pressure fluctuations over a stepped spillway with new step configuration. *Water Supply* **22**(7), 6321–6337.

Kramer, M., Hohermuth, B., Valero, D. & Felder, S. 2020 Best practices for velocity estimations in highly aerated flows with dual-tip phase-detection probes. *International Journal of Multiphase Flow* **126**, 103228.

Lopes, P., Leandro, J., Carvalho, R. F. & Bung, D. B. 2017 Alternating skimming flow over a stepped spillway. *Environmental Fluid Mechanics* **17**(2), 303–322.

Morovati, K. & Eghbalzadeh, A. 2016 Stepped spillway performance: Study of the pressure and turbulent kinetic energy versus discharge and slope. *Journal of Water Sciences Research* **8**(1), 63–77.

Muhsun, S. S., Al-Madhhachi, A. S. T. & Al-Sharify, Z. T. 2020 Prediction and CFD simulation of the flow over a curved crump weir under different longitudinal slopes. *International Journal of Civil Engineering* **18**(9), 1067–1076.

Nóbrega, J. D., Matos, J., Schulz, H. E. & Canelas, R. B. 2022 Smooth and stepped converging spillway modeling using the SPH method. *Water* **14**(19), 3103.

Pedersen, Ø., Fleit, G., Pummer, E., Tullis, B. P. & Rüther, N. 2018 Reynolds-averaged Navier-Stokes modeling of submerged ogee weirs. *Journal of Irrigation and Drainage Engineering* **144**(1), 04017059.

Puri, D., Sihag, P. & Thakur, M. S. 2023 A review: Aeration efficiency of hydraulic structures in diffusing DO in water. *MethodsX* **10**, 102092.

Ramya, N. S. & Kumar, N. S. 2023 Analysis and simulation of flow over stepped spillway using ANSYS-CFD. *Asian Research Journal of Current Science* **5**(1), 155–162.

Roushangar, K., Khowr, A. F., Saniei, M. & Alizadeh, F. 2020 Investigating impact of converging training walls of the ogee spillways on hydraulic performance. *Paddy and Water Environment* **18**, 355–366.

Roy, S. M., Jayraj, P., Machavaram, R., Pareek, C. M. & Mal, B. C. 2021 Diversified aeration facilities for effective aquaculture systems – a comprehensive review. *Aquaculture International* **29**, 1181–1217.

Saidin, M. S. I., Aziz, M. S., Zainol, M. R. R. M. A., Ishaik, M. H. H., Luo, P. & Malek, M. A. 2020 3D numerical investigation of water flow on unsymmetrical chute spillway. In: *AIP Conference Proceedings* (Rahim, S. Z. A., Saad, M. N. M., Al Bakri Abdullah, M. M., Tahir, M. F. M. & Mortar, M. A. M. (eds.)). Vol. 2291, No. 1. AIP Publishing. Seoul, South Korea.

Shahheydari, H., Nodoshan, E. J., Barati, R. & Moghadam, M. A. 2015 Discharge coefficient and energy dissipation over stepped spillway under skimming flow regime. *KSCE Journal of Civil Engineering* **19**, 1174–1182.

Srinivas, R. & Tiwari, N. K. 2022 Modeling of the oxygen aeration performance efficiency of gabion spillways. *Water Practice & Technology* **17**(11), 2317–2333.

Stojnic, I., Pfister, M., Matos, J. & Schleiss, A. J. 2021 Effect of 30-degree sloping smooth and stepped chute approach flow on the performance of a classical stilling basin. *Journal of Hydraulic Engineering* **147**(2), 4020097.

Tian, Y., Li, Y. & Sun, X. 2022 Study on the hydraulic characteristics of the trapezoidal energy dissipation baffle block-step combination energy dissipator. *Water* **14**(14), 2239.

Torrano, I., Tutar, M., Martinez-Agirre, M., Rouquier, A., Mordant, N. & Bourgoin, M. 2015 Comparison of experimental and RANS-based numerical studies of the decay of grid-generated turbulence. *Journal of Fluids Engineering* **137**(6), 061203.

Valero, D. & Bung, D. B. 2016 Development of the interfacial air layer in the non-aerated region of high-velocity spillway flows. Instabilities growth, entrapped air and influence on the self-aeration onset. *International Journal of Multiphase Flow* **84**, 66–74.

Wan, W., Raza, A. & Chen, X. 2019 Effect of height and geometry of stepped spillway on inception point location. *Applied Sciences* **9**(10), 2091.

Wang, H., Bai, Z., Bai, R. & Liu, S. 2022 Self-aeration of supercritical water flow rushing down artificial vegetated stepped chutes. *Water Resources Research* **58**(7), 2021WR031719.

Xu, W. L., Wang, Q. F., Wei, W. R., Luo, J. & Chen, S. Y. 2021 Effects of air bubble quantity on the reduction of cavitation erosion. *Wear* **482**, 203937.

Zawawi, M. H., Saleha, A., Salwa, A., Hassan, N. H., Zahari, N. M., Ramli, M. Z. & Muda, Z. C. 2018 A review: Fundamentals of computational fluid dynamics (CFD). In: *AIP Conference Proceedings* (Al Bakri Abdullah, M. M., Bin Abd Rahim, S. Z., Bin Mat Saad, M. N., bin Ghazi, Romisuhani Ahmad, M. F., Bin Mohd Tahir, M. F. & Jamaludin, L. B. (eds.)). Vol. 2030, No. 1. AIP Publishing, Ho Chi Minh, Vietnam.

Zhang, G. & Chanson, H. 2016 Hydraulics of the developing flow region of stepped spillways. I: Physical modeling and boundary layer development. *Journal of Hydraulic Engineering* **142**(7), 4016015.

First received 24 November 2023; accepted in revised form 4 February 2024. Available online 19 February 2024